

## QUANTITATIVE ENERGY-FILTERED CONVERGENT BEAM ELECTRON DIFFRACTION - MATCHING THEORY TO EXPERIMENT

M. Saunders<sup>1,2\*</sup>, P.A. Midgley<sup>1</sup>, T.D. Walsh<sup>1</sup>, E.S.K. Menon<sup>2</sup>, A.G. Fox<sup>2</sup> and R. Vincent<sup>1</sup>

<sup>1</sup>H.H. Wills Physics Laboratory, University of Bristol, Tyndall Avenue, Bristol, BS8 1TL, UK

<sup>2</sup>Center for Materials Science and Engineering, US Naval Postgraduate School, Monterey, California 93943, USA

### Abstract

Quantitative Convergent Beam Electron Diffraction (CBED) is now established as a means of accurate low-order structure factor determination. Using energy-filtered zone-axis CBED patterns it has been demonstrated that the 111 structure factor at the  $\langle 110 \rangle$  zone-axis in Si can be measured to better than 0.1%. In order to achieve this accuracy, it is essential to have a full understanding of the zone-axis pattern matching technique (ZAPMATCH) and the microscope system on which the data is acquired. Before any patterns can be analyzed, the effects of the detector system [in our case a Gatan Imaging Filter (GIF)] on the recorded intensities must be understood. Consideration must also be given to the number of structure factors that can be refined from any given data set. Our recent implementation of ZAPMATCH on a Topcon 002B with GIF provides an illustrative example of the former. Measurements of the low-order structure factors of nickel serve to demonstrate the latter.

**Key Words:** Quantitative Convergent Beam Electron Diffraction (CBED), structure factor, energy-filter, point spread function, noise model.

### Introduction

The measurement of low-order structure factors by quantitative Convergent Beam Electron Diffraction (CBED) techniques relies on the adjustment of a theoretical calculation until the best fit is obtained with an experimental data set (Bird and Saunders, 1992; Saunders *et al.*, 1995; Spence and Zuo, 1992). The variable parameters include a set of low-order structure factors, the sample thickness and some background and normalization terms. Two complementary strategies have developed based on the choice of diffraction geometry. Spence and Zuo (1992) and references therein, proposed the use of pseudo-systematic-row patterns whereas Bird and Saunders (1992) suggested an alternative approach using zone-axis patterns (the Zone-Axis Pattern MATCHing or ZAPMATCH technique). A number of papers have now been published explaining the principles of both techniques and establishing their success in making low-order structure factor measurements, for example Holmestad *et al.* (1995) and Saunders *et al.* (1995).

The accuracies achieved in the pattern matching calculations (with errors of less than 0.1%) are sufficient to study the redistribution of charge due to bonding effects in crystalline materials. Obtaining this accuracy is a non-trivial procedure. The quality of the CBED patterns required and the pre-processing involved prior to the pattern matching have been discussed previously in conference presentations. However, very little of this information is available generally for those wishing to pursue the technique.

For example, as the pattern matching techniques require an accurate set of diffracted intensities, it is necessary to understand how the detector system modifies these intensities during the acquisition process so that the effects of the detector can be removed from the data. The response of a Gatan Imaging Filter (GIF) attached to a Topcon (Tokyo, Japan) 002B has been studied. This includes the measurement of its point spread function (PSF) and the determination of a suitable noise model for the data. Preliminary results obtained from Ni  $\langle 110 \rangle$  data acquired on the same system are also discussed. This allows us to address the important question of how many structure factors one can measure from any given zone-axis pattern.

\*Address for correspondence:

M. Saunders  
Analytical Materials Physics, Ångström Laboratory  
Uppsala University  
Box 534, 75121 Uppsala, Sweden

Telephone number: +46-18-4717104

FAX number: +46-18-500131

E-mail: martin.saunders@angstrom.uu.se

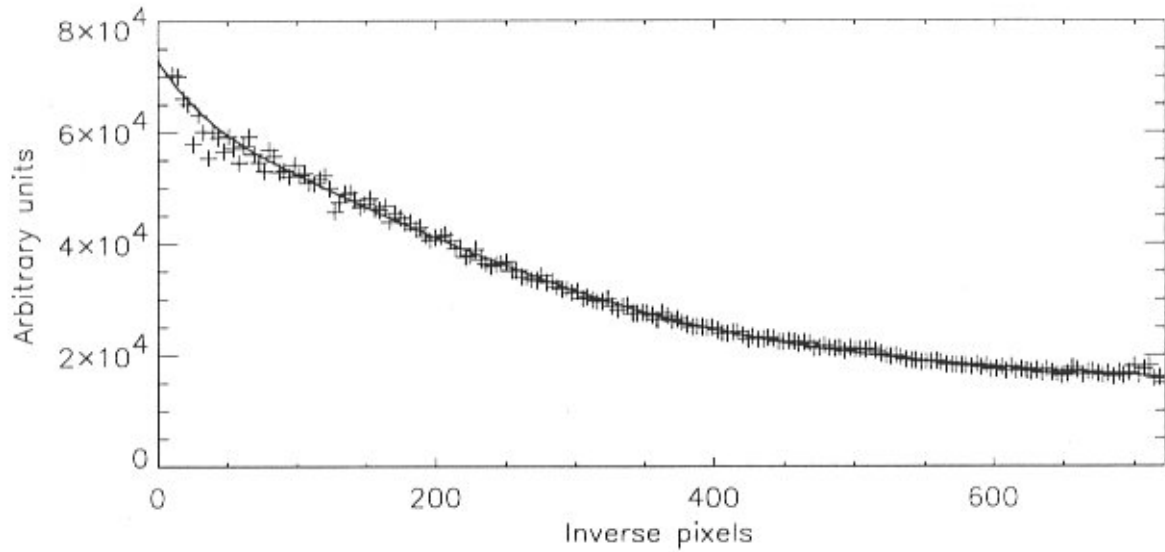


**Figure 1.** Plot of the modulation transfer function of the GIF determined experimentally using the “white noise technique” (de Ruiter and Weiss, 1992). The crosses represent the experimental data points. The line shows a spline curve interpolated from the experimental data (see text).

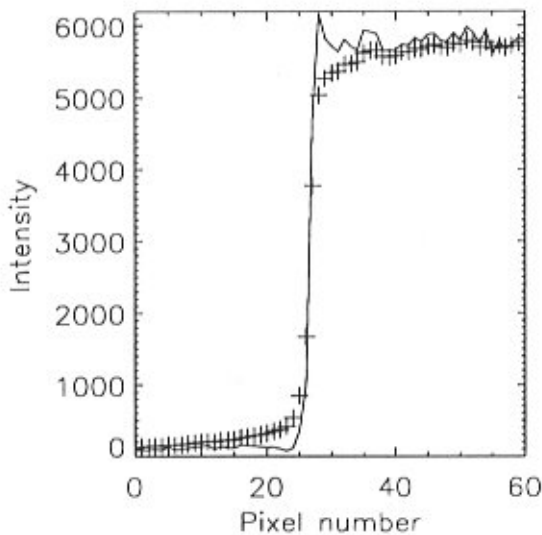


**Figure 2.** Line trace across the edge of an image of an aperture before deconvolution (crosses) and after deconvolution (line) with the MTF shown in Figure 1.

When using zone-axis patterns it is necessary to allow a number of low-order structure factors to vary in any given refinement calculation. However, due to the varying sensitivity of the pattern to the different structure factors, not all can be measured with sufficient accuracy to study bonding effects (~0.1%). Using the Ni <110> patterns as examples, the sensitivity of the patterns to different structure

factor parameters is investigated in order to determine how many structure factors can be refined from the <110> data.

#### Obtaining Quantitative Data

The best fit between the theoretical calculation and the experimental energy-filtered diffraction pattern is obtained by minimizing the sum-of-squares difference between the two data sets while adjusting a set of variable parameters. The sum-of-squares function used in the zone-axis pattern matching technique of Bird and Saunders (see for example, Saunders *et al.*, 1995) is given by

$$\chi^2 = \frac{1}{N_{data}} \sum_{i=1}^{N_{data}} \frac{(I_i^{ex} - cI_i^{th} - B_n)^2}{\sigma_i^2} \quad (1)$$

where the  $I^{ex}$  are the experimental intensities, the  $I^{th}$  are the theoretical intensities,  $c$  is a normalization coefficient, the  $B_n$  are a set of background levels, the  $\sigma^2$  are the variances of the experimental intensities and  $N_{data}$  is the total number of data points included in the fit.

To achieve the highest accuracy, there must be no contribution to the experimental intensities that cannot be modelled accurately by the theory. For example, the diffraction patterns must be energy-filtered to reduce the effects of inelastic scattering because the theory considers only elastic scattering (see, for example, Bird, 1989). Even using the GIF, it is not possible to remove inelastic effects completely due to the finite energy window of the collection system (~6 eV for these experiments). Thus, the constant

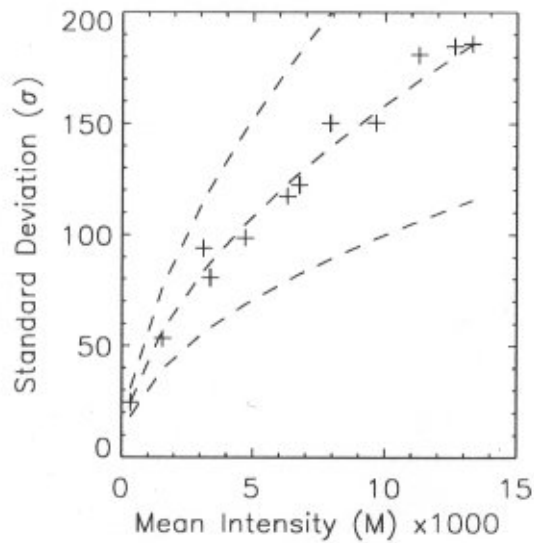


**Figure 3.** Plot of the standard deviation of the intensity ( $\sigma$ ) against the mean intensity ( $M$ ) for a series of deconvoluted white noise images. The experimental data point are shown as crosses. The curves represent Poisson noise (bottom), the previously measured curve for the Bristol system (top) and the best-fit for the NPS system (middle). See text for details.

terms  $B_n$  are an attempt to include the effects of the remaining inelastic background (mainly phonon scattering) in the theoretical model. It is assumed that the background is constant within a given disc and that symmetry related discs have the same background level. While this is clearly an over-simplification, experience has shown it to be sufficient provided thermal diffuse scattering is kept to a minimum, for example by cooling the sample or limiting its thickness. A better background model is currently being developed in an attempt to improve the fits even more.

In order to use the ZAPMATCH technique successfully it is essential that the detector system is well understood. The effects of the detector on the recorded intensities must be removed from the data before analysis and an appropriate noise model is required so that suitable values of  $\sigma_i$  can be used in equation (1). Recently we have acquired quantitative CBED patterns using a GIF attached to a Topcon 002B transmission electron microscope (TEM) with a LaB<sub>6</sub> source at the US Naval Postgraduate School (NPS), Monterey, California. The scintillator on the GIF is a YAG (yttrium aluminum garnet) with an anti-reflection coating. It is this system that we will consider in detail here.

It is well understood that the GIF has an associated PSF that tends to “blur” the patterns (see, for example, de Ruiter, 1995). This PSF is typically a Lorentzian-type

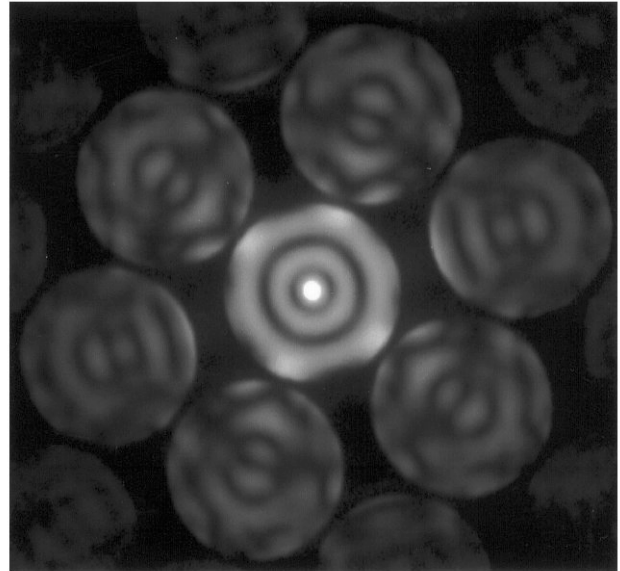


**Figure 4.** Energy-filtered Ni  $\langle 110 \rangle$  zone-axis CBED pattern (thickness  $\sim 1300 \text{ \AA}$ ) after deconvolution with the measured PSF of the detector. The data was acquired at  $196.7 \pm 0.2 \text{ kV}$  and room temperature with a probe size  $\sim 30 \text{ nm}$ .

function with a width of 3 or 4 pixels and long tails. It arises from two independent effects. First, there will be total internal reflection within the scintillator which accounts for the tails of the PSF. Second, below the scintillator is a set of fibre optic cables linking the scintillator to the CCD (charge-coupled device) detector. Coupling between these fibers is responsible for the central peak of the PSF. The effects of the detector PSF do not degrade severely the recorded diffraction pattern. *Qualitatively* the pattern will remain unaltered with all the major features still visible. However, because of the *quantitative* nature of our measurements it is important that the data we analyze is as close as possible to that which was incident on the scintillator. Thus we need to deconvolute the effects of the detector PSF from the recorded diffraction patterns. In order to do this we must first measure the PSF.

This is achieved using the “white noise method” described by de Ruiter and Weiss (1992). By recording white noise (we use a blank CBED disc with no sample) the image acquired by the GIF is the convolution of the white noise with the PSF. Taking the Fourier Transform (FT) of the image results in a pattern which is the multiplication of the FT of the PSF (called the modulation transfer function or MTF) with the FT of the white noise (which is also white noise). A rotational average of the Fourier transformed image about the origin produces a line profile in which the white noise has averaged out to reveal the true form of the MTF. Figure

1 shows a plot of the MTF obtained from the anti-reflection YAG on the GIF at NPS. The crosses indicate the experimental data points and the line shows a spline curve interpolated from this data. At both ends of the curve there is considerable error in the experimental data because of the small number of pixels used in the average. Thus, a certain amount of freedom is allowed in fitting the spline curve in these regions. This is particularly true close to the origin where the experimental data rises sharply before oscillating, whereas it is important to maintain a smooth variation in the fitted curve. This curve is rotated to create a two-dimensional MTF for deconvoluting experimental data. As a test, an image of a small aperture is deconvoluted. A line trace across the aperture should appear as a top hat function. Figure 2 shows a line trace across the edge of the aperture both before and after deconvolution. The success of the deconvolution indicates that the curve in Figure 1 is a good estimate for the MTF, and it is this criterion that is used in adjusting the fit to the points near the origin in Figure 1. An alternative to the white noise method is the “edge method” described by Weickenmeier *et al.* (1995) which, although more suited to measuring the tails of the PSF rather than the central peak, can be used to good effect for PSF measurements from a CCD detector.

It is often assumed that there is Poisson noise on the experimental data. Considering the fact that we are counting electrons incident on the detector this is an understandable assumption. Unfortunately, this is not completely accurate as the GIF processes the data so that the signal recorded by the detector does not have one-to-one correspondence with the electron count. In addition, patterns acquired with the GIF are normally corrected for the variable response of the scintillator and thermal noise in the detector. This data pre-processing alters the noise distribution such that the assumption of Poisson noise is no longer valid. In addition, the subsequent deconvolution of the detector PSF from the data also changes the noise distribution. We attempt to find a more suitable model for the noise by studying white noise images with a range of mean intensity values. Each image is deconvoluted with the experimentally determined PSF and a graph is plotted showing how the standard deviation of the intensities ( $\sigma$ ) varies with the mean intensity in the image ( $M$ ). Figure 3 shows such a plot for the GIF at NPS. The experimental data points are shown as crosses. The three curves represent the lines  $\sigma=M^{0.5}$  (Poisson noise),  $\sigma=M^{0.59}$  (for the GIF at Bristol) and  $\sigma=M^{0.55}$  (for the GIF at NPS). Clearly the last curve gives a suitable match for the NPS system. This means that the variance of the experimental intensities in (1) which is  $\sigma^2$  is given by  $(I^{ex})^{1.1}$ . Now that a realistic noise model has been found, the values of  $\chi^2$  obtained from (1) in the pattern matching calculations are more easily interpreted. A perfect noise limited fit will give a value of unity. As the variance  $\sigma^2$

in (1) is effectively acting as a weighting parameter, the use of a less accurate noise model results in a less accurate fit biased in favor of either the higher or lower-end intensities.

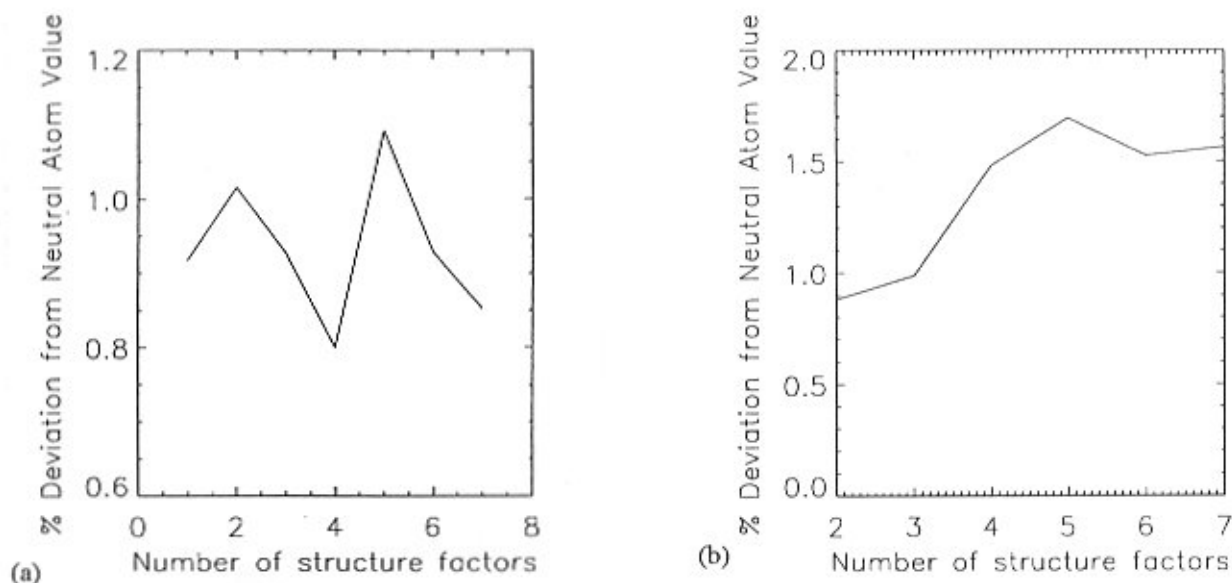
### How Many Structure Factors Can Be Refined from a Single Zone-Axis Pattern?

Figure 4 shows an energy-filtered Ni  $\langle 110 \rangle$  zone-axis pattern (sample thickness  $\sim 1300 \text{ \AA}$ ) acquired on the Topcon 002B at NPS. The PSF of the detector has already been deconvoluted from the raw data. The microscope accelerating voltage has been measured to be  $196.7 \pm 0.2 \text{ kV}$ , the probe size is  $\sim 30 \text{ nm}$  and the data was acquired at room temperature (where a Debye-Waller factor of  $0.4 \text{ \AA}^2$  is assumed, as given by Fox and Fisher, 1988). As in previous studies of Si  $\langle 110 \rangle$  patterns (Saunders *et al.*, 1995, 1996), data for the pattern matching calculations is taken from the seven innermost reflections, i.e., the bright field,  $\{111\}$  and  $\{002\}$  discs. A decision must be made as to which structure factors the pattern is sensitive. This choice has two aspects. First, how many structure factors must be included as variable parameters in the fit? Second, how many of these are we likely to measure with sufficient accuracy to study bonding effects ( $\sim 0.1\%$ )?

In the silicon work, the six lowest-order structure factors were allowed to vary, i.e., out to  $\{331\}$ . The reasoning behind this was that the pattern should be sensitive to at least all structure factors that cause scattering between the discs for which we have data (in this case out to  $\{004\}$  which links the two  $\{002\}$  reflections). The  $\{331\}$  is included in an effort to absorb errors due to any additional terms to which the pattern is sensitive which we have chosen to omit from the fit. While this gave very successful results for silicon, it is a rather simplistic way of looking at the sensitivity question without any formal basis. The results also indicated that the highest sensitivity was achieved for reflections into which scattering could occur directly from the bright field disc, i.e. only  $\{111\}$  in this case as  $\{002\}$  is kinematically forbidden. As we chose to include only data from reflections out to  $\{002\}$  then all of the other structure factors can only contribute by multiple scattering routes which appears to reduce the sensitivity of the pattern to them.

In our studies of Ni  $\langle 110 \rangle$  patterns we have tried to address the question of sensitivity in a different way. Fits have been run with different numbers of structure factor variables for the pattern shown in Figure 4. Structure factors which are not allowed to vary are fixed at their neutral atom values (Doyle and Turner, 1968). This means that any contributions to the bonding from these structure factors are ignored. If the pattern is sufficiently sensitive to some of the lost contributions to the scattering potential then one might expect to see the structure factors that are allowed





**Figure 5.** Percentage deviation from neutral atom electron structure factors for (a) 111 and (b) 002 structure factors of nickel for repeated fits with varying numbers of structure factors included in the fit (see text).

to vary compensating in some way for the loss of information. It is this reaction to the lost bonding terms that we hope to observe in our calculations. The first fit is run with the {111}, {002}, {220}, {113}, {222}, {004} and {331} structure factors allowed to vary. The fit is repeated six times, each with one less structure factor variable. The fitting calculations include 137 beams in an exact diagonalisation of the many-beam matrix with a further 200 beams included as Bethe potentials. As in our previous work with zone-axis patterns (for example, Saunders *et al.*, 1995) we have chosen to omit HOLZ (High-Order Laue Zone) reflections from the calculation in the belief that they do not significantly effect the intensities used for the pattern matching calculations at this axis.

Figure 5 shows plots of the percentage change in the {111} and {002} electron structure factors ( $U_g$ ) from their neutral atom values for the fits run with 1 to 7 structure factors. The {111} structure factor appears insensitive to the removal of information from the calculation demonstrating that it can be measured with high accuracy from this pattern. The {002} structure factor converges to a settled value when 5 or more structure factors are allowed to vary suggesting that this is a suitable number of variables for the fitting calculations. With fewer variables, the {002} structure factor appears to compensate for the errors introduced by fixing the higher-order terms in the potential at their neutral atom values. The corresponding plots for the other structure factors (not shown here) demonstrate such large scatter that we are unlikely to measure them with

sufficient accuracy to determine bonding effects at this axis using data from only reflections out to {002}. Thus, it is suggested that bonding measurements are only possible for structure factors corresponding to reflections from which diffraction data has been collected [as has already been observed by Spence and Zuo (1992) in the pseudo-systematic geometry]. However, it appears that additional structure factors must be allowed to vary as part of the fit in order to ensure that the lowest-order structure factors are able to find their optimum values though the errors in these higher-order terms (generally  $\sim 0.5\%$ ) are insufficient to study bonding. We have therefore chosen to run all subsequent fits with 5 structure factor variables, i.e., those out to {222}, with the intention of measuring the {111} and {002} structure factors with sufficient accuracy to study bonding effects.

Table 1 shows the results of the pattern matching calculation from the data set shown in Figure 4. They are compared to results obtained previously from critical voltage measurements (Fox and Fisher, 1988) and unpublished ZAPMATCH data we have obtained using a Hitachi (Tokyo, Japan) HF2000 field emission gun (FEG)-TEM with GIF at Bristol. The agreement is excellent indicating that the measurements of the detector function described earlier have been successful and that our choice of the number of variable parameters in the fit is sensible. The errors in the fitted measurements are indicated in parenthesis. The error analysis carried out here is similar to that given in Bird and Saunders (1992) where contributions to the error from

**Table 1.** Measured low-order structure factors of nickel.

Structure Factor	Neutral Atom	Critical Voltage	ZAPMATCH (Bristol unpub.)	ZAPMATCH (This paper)
111	20.537	20.482	20.49(1)	20.49(2)
002	19.240	19.181	19.18(2)	19.20(2)

A comparison is shown between neutral atoms (Doyle and Turner, 1968), critical voltage measurements (Fox and Fisher, 1988), previous ZAPMATCH measurements (Saunders *et al.*, unpublished) and the results obtained from the patterns shown in Figure 4. Values are quoted in electrons/atom at room temperature ( $a_0=3.524 \text{ \AA}$ ) and the Debye-Waller factor contribution (where  $B=0.40 \text{ \AA}^2$ ) has been stripped from the measured electron structure factor.

uncertainties in the lattice parameter, accelerating voltage and Debye-Waller factor have been considered. Almost all of the errors given in Table 1 result from the assumed uncertainty of  $\pm 5\%$  in the Debye-Waller factor.

### Conclusions

Given an understanding of the data acquisition and how to obtain truly quantitative diffraction intensities, it is possible to make very accurate structure factor measurements. Where it is not possible to include an effect in the theoretical model (for example the PSF of the GIF) every effort must be made to remove it from the experimental data prior to the pattern matching calculation. With care, accurate models can be found for both the PSF and the noise distribution on the data, thus enhancing the accuracy of the structure factor measurements.

The choice of the number of structure factors to include as variables in the fit is an important one. First, the set of low-order structure factors to which the pattern is sensitive must be found. Second, results indicate that it is only a sub-set of these parameters that one can expect to measure with the accuracy required to study bonding effects ( $\sim 0.1\%$ ). A simplistic argument is to suggest that the highest accuracy should be obtained for those structure factors corresponding to reflections from which diffraction data is collected for the fit (as is exploited by Spence and Zuo (1992) in their pseudo-systematics patterns). Our results from Ni  $\langle 110 \rangle$  data where a data-set including the bright field,  $\{111\}$  and  $\{002\}$  reflections has allowed us to measure the  $\{111\}$  and  $\{002\}$  structure factors further enhance this belief. However, further studies are required to investigate the behavior of patterns acquired at a range of sample thicknesses in order to confirm whether this simplistic model is generally applicable.

### Acknowledgements

Some of the data discussed in this paper was

acquired during a visit by two of the authors (M.S. and P.A.M.) to the US Naval Postgraduate School in Monterey, California. We are grateful to Dr. Atul Kumar for his assistance during this time. The support of the Engineering and Physical Sciences Research Council (EPSRC) is also acknowledged. M.S. would also like to thank Lt. Mike Greene and Mr. Rich Hashimoto for their assistance in the preparation of this manuscript.

### References

- Bird DM (1989) Theory of zone axis electron diffraction. *J Electron Microscop Tech* **13**: 77-97.
- Bird DM, Saunders M (1992) Sensitivity and Accuracy of CBED Pattern Matching. *Ultramicroscopy* **45**: 241-251.
- De Ruiter WJ (1995) Imaging properties and applications of slow-scan charge-coupled device cameras suitable for electron microscopy. *Micron* **26**: 247-275.
- De Ruiter WJ, Weiss JK (1992) Methods to measure properties of slow-scan CCD cameras for electron detection. *Rev Sci Instrum* **63**: 4314-4321.
- Doyle PA, Turner PS (1968) Relativistic Hartree-Fock X-ray and electron scattering factors. *Acta Cryst* **A24**: 390-397.
- Fox AG, Fisher RM (1988) A Summary of low-angle X-ray atomic scattering factors measured by the critical voltage effect in high energy electron diffraction. *Aust J Phys* **41**: 461-468.
- Holmestad R, Zuo JM, Spence JCH, Høier R, Horita Z (1995) Effect of Mn doping on charge density in  $\gamma$ -TiAl by quantitative Convergent Beam Electron Diffraction. *Phil Mag A* **72**: 579-601.
- Saunders M, Bird DM, Zaluzec NJ, Burgess WG, Preston AR, Humphreys CJ (1995) Measurement of low-order structure factors for silicon from zone-axis CBED patterns. *Ultramicroscopy* **60**: 311-323.
- Saunders M, Midgley PA, Vincent R, Steeds JW (1996) Recent advances in quantitative Convergent Beam

Electron Diffraction. *J Electron Microsc* **45**: 11-18.

Spence JCH, Zuo JM (1992) *Electron Microdiffraction*. Plenum, New York. Chapter 4.

Weickenmeier AL, Nüchter W, Mayer J (1995) Quantitative characterization of point spread function and detection quantum efficiency for a YAG scintillator slow scan CCD camera. *Optik* **99**: 147-154.

### Discussion with Reviewers

**R. Holmestad:** You say that the {220}, {113}, {222} and {004} structure factors are impossible to measure with sufficient accuracy; but still they have to be varied to get the lower-order ones to converge. Isn't this a contradiction?

**D.M. Maher:** In the refinements five structure factors, including {111} and {002}, have to be varied in order to ensure convergence in {002}. The role of the three additional structure factors is not clear!

**J.M. Zuo:** Why are higher order reflections varied when only low orders are measured? Could the variation in the high orders compensate for systematic errors?

**Authors:** The important factor here is the *sensitivity* of the diffracted intensities to the various structure factors. We have stated from the outset that our aim is to make structure factor measurements with sufficient accuracy to study bonding effects. This necessitates reducing the errors in the refined structure factor values to of order 0.1%. In the case of the nickel zone-axis CBED patterns considered in this paper, it is only the {111} and {002} structure factors that can be retrieved with sufficient accuracy for bonding studies and thus, it is only those values that we have given in Table 1. The sensitivity of the data to the {220}, {113} and {222} structure factors is lower than that observed for the {111} and {002} terms making it impossible for us to accurately measure bonding effects from them. However, there is sufficient sensitivity that we do need to allow them to vary as part of the fit, i.e. fixing them at their neutral atom values would introduce systematic error into the {111} and {002} structure factors. In our opinion, evidence of this systematic error effect is shown in Figure 5b where a reduction in the number of variables included in the fit is seen to reduce the accuracy of the refined {002} structure factor value in a systematic way.

This question of how many variables are required and how many of those variables can be recovered with the desired accuracy is still one that needs further consideration. We are in the process of conducting further experiments with the aim of producing a set of semi-empirical rules for use in future calculations. While the initial results of this work are encouraging, at the time this paper goes to press the project remains incomplete. It is our intention to address this question again in future papers.